Individual hematopoietic stem cells in human bone marrow of patients with aplastic anemia or myelodysplastic syndrome stably give rise to limited cell lineages

著者	Katagiri Takamasa, Kawamoto Hiroshi, Nakakuki Takashi, Ishiyama Ken, Okada-Hatakeyama Mariko, Ohtake Shigeki, Seiki Yu, Hosokawa Kohei, Nakao Shinji
journal or publication title	Stem Cells
volume	31
number	3
page range	536-546
year	2013-03-01
URL	http://hdl.handle.net/2297/34136

doi: 10.1002/stem.1301

Individual hematopoietic stem cells in human bone marrow of patients with aplastic anemia or myelodysplastic syndrome stably give rise to limited cell lineages

Short title: HSCs produce limited cell lineages

Takamasa Katagiri[1)2)*], Hiroshi Kawamoto[3)*], Takashi Nakakuki[4)*], Ken Ishiyama[2)], Mariko Okada-Hatakeyama[5)], Shigeki Ohtake[1)], Yu Seiki[2)], Kohei Hosokawa[2)] and Shinji Nakao[2)]

[1)] Clinical Laboratory Science, Division of Health Sciences, Kanazawa University Graduate School of Medical Science, 5-11-80 Kodatsuno, Kanazawa, Ishikawa 920-0942 Japan.
[2)] Cellular Transplantation Biology, Kanazawa University Graduate School of Medical Science, 13-1 Takara-machi, Kanazawa, Ishikawa 920-8640 Japan.
[3)] Laboratory for Lymphocyte Development, RIKEN Research Center for Allergy and Immunology, 1-7-22 Suehiro-cho, Tsurumi-ku, Yokohama, Kanagawa 230-0045 Japan.
[4)] Department of Mechanical Systems Engineering Faculty of Engineering, Kogakuin University, 1-24-2 Nishishinjuku, Shinjuku-ku, Tokyo 163-8677 Japan
[5)] Laboratory for Cellular Systems Modeling, RIKEN Research Center for Allergy and Immunology, 1-7-22 Suehiro-cho, Tsurumi-ku, Yokohama, Kanagawa 230-0045 Japan.

* T.K., H.K. and T.N. were equally contributed to this work.

Corresponding to:
Shinji Nakao (snakao8205@staff.kanazawa-u.ac.jp)
Cellular Transplantation Biology, Kanazawa University Graduate School of Medical Science, 13-1 Takara-machi, Kanazawa, Ishikawa 920-8640 Japan.

Abstract

Mutation of the *PIG-A* gene in hematopoietic stem cells (HSCs) results in the loss of glycosylphosphatidylinositol-anchored proteins (GPI-APs) on HSCs, but minimally affects their development, and thus can be used as a clonal maker of HSCs. We analyzed GPI-APs expression on six major lineage cells in a total of 574 patients with bone marrow (BM) failure in which microenvironment itself is thought to be unaffected, including aplastic anemia (AA) or myelodysplastic syndrome (MDS).

GPI-APs-deficient (GPI-APs$^-$) cells were detected in 250 patients. Whereas the GPI-APs$^-$ cells were seen in all six lineages in a majority of patients who had higher proportion ($\geqq$3%) of GPI-APs$^-$ cells, they were detected in only limited lineages in 92.9% of cases in the lower proportion (<3%) group. In all 250 cases, the same lineages of GPI-APs$^-$ cells were detected even after 6-18 month intervals, indicating that the GPI-APs$^-$ cells reflect hematopioesis maintained by a self-renewing HSC in most of cases. The frequency of clones with limited lineages seen in mild cases of AA was similar to that in severe cases, and clones with limited lineages were seen even in two health volunteer cases. These results strongly suggest most individual HSCs produce only restricted lineages even in a steady state. While this restriction could reflect

heterogeneity in the developmental potential of HSCs, we propose an alternative model in which the BM microenvironment is mosaic in supporting commitment of progenitors towards distinct lineages. Our computer simulation based on this model successfully recapitulated the observed clinical data.

Introduction

To sustain hematopoiesis, hematopoietic stem cells (HSCs) must, on the one hand, replenish themselves by self-renewal and on the other hand produce differentiating progenitor cells. It is also known that most HSCs remain dormant and are only rarely and randomly activated. It has been estimated that each human possesses a total of 10^4 HSCs, and that ~400 HSCs actively contribute to hematopoiesis, replicating once per year[1, 2]. However, the actual dynamics of hematopoiesis by HSCs remains uncertain. For example, it is unclear how long an individual HSC maintains hematopoiesis and whether all major lineage cells are produced from a single HSC. These issues have been difficult to address due to the lack of appropriate experimental systems, regardless of animal species.

In the case of humans, however, we were led to consider one “experiment of nature” that makes it possible to track the progeny of a HSC; i.e. by detecting blood cells

deficient in glycosylphosphatidylinositol-anchored proteins (GPI-APs) using flow cytometry. GPI-APs-deficient (GPI-APs$^-$) blood cells are rarely detectable in healthy individuals, but are a common feature in paroxysmal nocturnal hemoglobinuria (PNH) and are also frequently seen in patients with bone marrow (BM) failure such as AA or MDS. These cells are known to be derived from HSCs with a mutation in the phosphatidylinositol N-acetylglucosaminyltransferase subunit A (*PIG-A*) gene. MDS cases harboring GPI-APs$^-$ blood cells are characterized by polyclonal hematopoiesis and good response to immunosuppressive therapy, and are therefore thought to be similar to AA in their pathophysiology[3].

The *PIG-A* mutant HSCs used to be thought to have greater proliferative capacity than normal HSCs because one or a few *PIG-A* mutant clones sometimes account for a large proportion of hematopoietic cells for long period in PNH patients[4]. However, several reports instead indicate that the mutant HSCs in most PNH patients have properties similar to normal HSCs: e.g. no growth advantage over wild-type HSCs[5,6], genetic stability and extremely low incidence of secondary mutations[2, 7-9], and the rarity of leukemic cell evolution of GPI-APs$^-$ cells in PNH patients[10].

We recently found that GPI-APs$^-$ cells in patients with AA and MDS frequently show various patterns in the proportion of granulocytes and erythrocytes and that the

individual patterns of the two lineage combinations can persist for many years. The percentage of GPI-APs$^-$ cells in some patients remained almost the same over 10 years even when the percentages were less than 1%[11]. In such stable cases, it is quite likely that GPI-APs$^-$ peripheral blood cells are produced from HSC(s), and that the GPI-APs$^-$ HSC itself as well as its surrounding environment is largely normal, at least during the observation period. Indeed, BM environment itself in the patients to support hematopoiesis is thought to be largely normal, since these cases are thought to be caused by immune reaction against blood cells. It is also highly probable that the whole GPI-APs$^-$ cells in each patient represent a clone, originating from a single HSC in which *PIG-A* mutation occurred, since it is statistically rare that the *PIG-A* mutation occurs twice in one patient. Although it is unclear that such a clone is maintained by a single HSC or multiple descendent HSCs, it can be said that the kinetics of GPI-APs$^-$ cells during stable period reflect the regular hematopoietic events originally initiated by a single HSC. We then thought that it could be very much informative if we extend our analysis to cover various hematopoietic lineages in addition to erythrocytes and granulocytes. We therefore determined the proportion of GPI-APs$^-$ cells in six major lineages, namely granulocytes (G), monocytes (M), erythrocytes (E), T cells (T), NK cells (NK) and B cells (B), in peripheral blood (PB) cells from BM failure patients

using a highly sensitivity flow cytometric analysis[12].

Materials and Methods

Patients and healthy volunteers

The PB of 574 patients with various types of cytopenias was examined for the presence of GPI-APs$^-$ cells using high sensitivity flow cytometry. Their diagnoses included AA in 354 (39 with very severe, 92 with severe, and 223 with non-severe AA[13]), MDS-refractory anemia (RA) defined by the FAB classification[14] in 207, and classic PNH in 13. The male to female ratio was 1: 1.2 (261:313) and the median age was 57 years (range: 1 to 95 years). PB samples from 192 healthy individuals were also examined for the presence of GPI-APs$^-$ cells in all lineages of cells. All patients and healthy individuals including next of kin on the behalf of minors/ children participants in our study provided their informed written consent before sampling. This study protocol was approved by the ethics committee of Kanazawa University Graduate School of Medical Science.

Monoclonal antibodies (mAbs)

mAbs used for multicolor flow cytometry were; anti-CD59 labeled with FITC (P282E,

IgG2a; Beckman Coulter, Miami, FL), anti-CD55 labeled with FITC (IA10, IgG2a; BD Pharmingen), anti-CD48 labeled with FITC (J4-57, IgG1; Beckman Coulter), anti-CD33 labeled with APC (D3HL60.251, IgG1; Beckman Coulter), anti-CD19 labeled with APC-Cy7 (SJ25C1, IgG1; BD Pharmingen), anti-CD335 labeled with PE (BAB281, IgG1; Beckman Coulter), anti-CD3 labeled with PerCP-Cy5.5 (SK7, IgG1; BD Pharmingen), anti-CD11b/Mac-1 labeled with PE (ICRF44, IgG1; BD Pharmingen), anti-glycophorin A labeled with PE (JC159, IgG1; Dako, Carpenteria, CA).

Flow cytometry for detecting GPI-APs$^-$ cells

Six lineages of blood cells including granulocytes, erythrocytes, monocytes, T cells, B cells and NK cells were subjected to high sensitivity flow cytometry for detecting small populations of GPI-APs$^-$ cells. All blood samples were analyzed within 24 h to avoid false positive results due to cell damage. The staining with the each mAb in this study was performed according to the well-established lyse-stain protocol, previously described in detail[12, 15]. Briefly, 3 to 5 mL of heparinized blood was drawn from the patients and healthy individuals. Erythrocytes were lysed in a lysis buffer containing NH_4Cl 8.26 g/L, $KHCO_3$ 1.0 g/L, and EDTA · E4Na 0.037 g/L to detect GPI-APs$^-$ leukocytes. After washing with saline, 50 µL of the leukocyte suspension was

incubated with FITC-labeled anti-CD55 and anti-CD59 mAbs for granulocytes or FITC-labeled anti-CD48 and anti-CD59 mAbs for monocytes, T cells, B cells and NK cells in combination with mAbs specific for lineage markers including PE-labeled CD11b for granulocytes, APC-labeled CD33 for monocytes, PerCP-Cy5.5 labeled CD3 for T cells, APC-Cy7 labeled CD19 for B cells and PE labeled CD335 for NK cells. Fresh blood was diluted to 3% in phosphate-buffered saline (PBS), and then 50 µL was incubated with PE-labeled anti-glycophorin A and FITC-labeled anti-CD55 and anti-CD59 mAbs on ice for 30 minutes to detect GPI-APs^{-} erythrocytes. Three-step gating excluded debris and immature granulocytes that are frequently found in samples from patients with MDS. Step 1 involved the gating of granulocyte, lymphocyte or monocyte populations from the FSC-SSC scattergrams (R1). Step 2 involved the gating of the lineage marker^{bright} population on the lineage marker-SSC scattergram to exclude the lineage marker^{dim} cells that are features of either damaged cells or immature cells. Step 3 was the gating of R1 × R2 and the analysis of 10^6 cells on R1 × R2 scattergrams. The following cut-off values that had been determined by our previous studies based on 183 healthy individuals were used; the presence of ≥0.005% $CD55^{-}CD59^{-}$ glycophorin A^{+} erythrocytes, ≥0.003% $CD55^{-}CD59^{-}CD11b^{+}$ granulocytes, and ≥0.01% $CD48^{-}CD59^{-}$ $CD33^{+}$ monocytes, $CD48^{-}CD59^{-}$ $CD3^{+}$ T cells, $CD48^{-}CD59^{-}CD19^{+}$ B

cells and $CD48^{-}CD59^{-}CD335^{+}$ NK cells [12, 16]. When GPI-APs^{-} cells were detected in only one lineage of cells or the percentages of GPI-APs^{-} cells were less than 0.01%, then additional samples were tested, and the patients were judged to be positive for increased GPI-APs^{-} (PNH^{+}) when the analysis results of the first and second samples were identical.

Data acquisition was performed immediately after the sample preparation using a FACSCanto II® instrument (Beckton Dickinson) and the data were analyzed using the FACSDiva software program and the percentage of each population was calculated by FlowJo software 7.6.1 (Tree star, Inc. Ashland, OR).

Cell sorting and *PIG-A* gene analysis

Freshly isolated GPI-APs^{-} cells were separated from GPI-APs^{+} fraction using a FACSAria II® instrument (Beckton Dickinson). More than 95% of the sorted cells were GPI-APs deficient. An analysis of the *PIG-A* gene mutation was performed as described previously[17]. Briefly, the coding regions of *PIG-A* were amplified by nested or semi-nested PCR using 12 primer sets, and 6 ligation reactions were used to transform competent Escherichia coli JM109 cells (Nippon Gene, Japan). Five clones were selected randomly from each group of transfectants and subjected to sequencing with

BigDye Terminator v3.1 Cycle Sequencing kit (Applied Biosystems, San Diego, CA) and an ABI PRISM 3100 Genetic Analyzer (Applied Biosystems).

Simulation of the blood cell production by HSCs

Migration, division, lineage determination and death of clones of a HSC in BM environment are simulated with a lattice Monte Carlo method. For efficient simulation, we focused on the events on a cross-section of BM, which enabled us to perform two-dimensional simulation. The occurrence of events was managed with their transition probabilities and the simulation was executed on the basis of actual time. We employed the hybrid null-event Monte Carlo algorithm[18, 19], and here outline the model description and simulation setup (Also see ***Supplementary Note*** for detailed information). A square area (30 mm×30 mm) that is large enough to encompass some commitment planes is represented using 1500×1500 square lattices (20 μm×20 μm each). Initially, a HSC is randomly added to a site, and then it continues to create clones once per 10 hours until there have been five divisions. Clones randomly move along the lattice with the transition probability, and undergo cell division once per 8-12 hours. We assume that lineage determination occurs after the fifth division, based on the site of the clone in the mosaic-like hematopoietic environment where each site supports

differentiation into M, E, B or T cell lineages. In addition, the lineage clone becomes a mature cell after a further five divisions under the condition that it can divide only in the sites that support differentiation into the same lineage. Otherwise cell death results after 48-hour movement on areas that support other lineages, although all clones die 72 hours after maturation.

We also investigated the relation between clone size and the number of emerging cell lineages. In our simulation, clone size is dominated by the setting of "*N* times divisions for lineage determination and further *N* times divisions for maturing". We simply change the number *N* in a range of 3-12. For each *N*, 128 simulations starting from randomly selected initial sites of HSCs are executed for 120 simulation hours. For each simulation, the number of cell lineages is counted, and clone size is calculated as the maximum number of clones for the entire simulation period.

Results

GPI-APs$^-$ cells were seen in various combination of lineages of blood cells from BM failure patients

Of 574 patients with BM failure, GPI-APs$^-$ cells were detected in at least one lineage of cells of 250 patients (44%). The prevalences of increased GPI-APs$^-$ cells were 56% in

AA and 19% in MDS-RA. The proportion of GPI-APs$^-$ cells among granulocytes ranged 0.003% to 99.1%, with mean and median value 5.38% and 0.19% respectively. GPI-APs$^-$ cells were rather frequently found in patients with less severe AA; the prevalences were 63% in non-severe, 49% in severe, and 31% in very severe AA patients. The lineage combinations of GPI-APs$^-$ cells in patients possessing GPI-APs$^-$ cells (PNH$^+$ patients) were classified into 16 different patterns (Supplementary Table 1). Figure 1 shows representative flow cytometric profiles of one healthy individual and 4 patients showing GMETNKB, GME, GMETNK or GMEB patterns.

Clone size of GPI-APs$^-$ granulocytes correlates with the number of cell lineages that contain GPI-APs$^-$ cells

The percentages of GPI-APs$^-$ granulocytes in each group bearing GPI-APs$^-$ cells in 1 to 6 lineages are plotted in Figure 2. There was a clear trend toward the pattern of the higher the percentage of GPI-APs$^-$ granulocytes in patients, the greater the number of GPI-APs$^-$ cell lineages.

In order to closely examine the relationship between the severity of AA and the GPI-APs$^-$ clone size, we arbitrarily classified AA patients in this study into five categories, namely stage 1, 2 and 3 (non severe) , stage 4 (severe), and stage 5 (very

severe), based on the severity of cytopenias (Supplementary Table 2) and replotted the data (Figure 2B). Patients with higher proportion (>1%) of GPI-APs$^-$ granulocytes were not seen in non severe cases, suggesting that the clone size of GPI-APs$^-$ cells correlates with severity of BM failure. The notable observation here is that the correlation between the percentage of GPI-APs$^-$ granulocytes and the number of GPI-APs$^-$ cell lineages is almost identical in all three groups. This finding may indicate that the production of limited lineage cells observed in smaller clones is not due to the possible functional failures of BM microenvironment. It seems more likely that “fewer lineages in smaller clones” instead represents events occurring in normal hematopoiesis.

Persistence of GPI-APs$^-$ lineage combination over a long period

We then reexamined PB cells of 250 patients 6 to 18 months after the first examination and to our surprise, GPI-APs$^-$ cells were observed in all 250 patients. Detection of GPI-APs$^-$ cells after such a long interval indicates that the GPI-APs$^-$ cells are most likely derived from HSCs rather than from non-self-renewing progenitors. Of special interest was our finding that in all 250 cases, the same combinations of lineages were detected regardless of the interval between the first and second analysis. Flow cytometric profiles of various lineages of a case representing GMET type are shown in

Figure 3. Figure 4 shows the proportion of GPI-APs$^-$ cells in each lineage in the first and second analysis for a total of representative 25 cases (5 cases for each type).

PIG-A gene mutations in different lineages of blood cells

To confirm their clonal origin, GPI-APs$^-$ cells sorted from 5 patients were subjected to *PIG-A* gene analysis. The same mutation was identified in different lineages in 3 patients (Supplementary Table 3). In GPI-APs$^-$ granulocytes with other lineages from Patients 16, 1 and 5 and GPI-APs$^-$ granulocytes from Patients 9 and 30, the same mutation was found 3 to 7 months after the initial analyses. Therefore, it is highly probable that in most, if not all, cases the GPI-APs$^-$ cells are clonal[20]. This finding is in line with the estimation that PNH patients only rarely have more than two clones at the HSC level[8, 9].

GPI-APs$^-$ cells were detected in limited lineages in healthy volunteers over a long period

Dormant HSCs with *PIG-A* mutation reside in the BM and can be activated albeit uncommonly[17]. If this hypothesis is tenable, small populations of GPI-APs$^-$ cells may be detectable in some healthy individuals. We then examined PB of 192 healthy volunteers

for the presence of GPI-APs$^-$ cells. Notably, two were found to bear detectable levels of GPI-APs$^-$ cells, and in both of them GPI-APs$^-$ cells were detected in limited lineages, representing GME and GE type (Figure 5A). The two healthy cases bearing GPI-APs$^-$ cells were situated within the range of distribution of AA and MDS cases in terms of chimerism ratio vs. lineage number (Figure 5B), further supporting that findings seen in AA and MDS cases reflect normal hematopoiesis.

As described in Introduction section, the number of active human HSCs at any given time is estimated to be around 400. It is therefore likely that the GPI-APs$^-$ clones with a frequency of less than 0.25% reflect hematopoiesis maintained by a single HSC. It is clear from our studies that most of these small clones contain only limited lineage cells. Even in the case of larger clones, e.g. clones of 1-3% chimerism that might be maintained more than two HSCs, the majority (81%) are non-full-lineage clones. Collectively, these results indicate that most individual human HSCs only give rise to a limited range of hematopoietic progeny.

A model for the hematopoietic microenvironment to explain the production of limited cell lineages from a HSC

A cogent explanation for this phenomenon may have important implications for normal

hematopoiesis. We considered several possible explanations such as; (a) the limited lineage spectrum of progeny cells may reflect the presence of progenitors with equally limited potential, (b) HSCs are intrinsically heterogeneous in terms of developmental potential, (c) BM environment is heterogeneous in its ability to support the differentiation of distinct lineages. However, as will be discussed later, these cases seemed quite unlikely.

Instead of above ideas, we came to think that the unexpected production of limited cell lineages by HSCs may be explained by assuming the presence of mosaic-like hematopoietic environments that can differently support the “commitment” of early multipotent progenitors to a certain lineage.

We attempted to test this idea by modeling and simulation. For simplicity, granulocytes and monocytes are placed into the myeloid lineage while T and NK cells are placed into the T lineage, consequently all lineages being classified into M, E, T, B lineages. The clinically observed data for chimerism ratio and detected lineages shown in Figure 2A are re-plotted in Figure 6A. For cases where the proportion of GPI-APs$^-$ clones is between 0.3 and 3% (representing typical size clones), the frequencies of different lineage combinations are shown in Figure 6B.

We assume that a self-renewing HSC is located in a particular location in BM and

that uncommitted progenitors derived from this HSC can reach to a certain defined area (Figure 6C), which we term here the “commitment sphere” (see also ***Supplementary Note*** for detailed information). If the BM microenvironment is mosaic in terms of function in inducing the commitment of progenitors towards a certain lineage, and the size of such mosaic is as large as commitment sphere, then production of progenitors of limited lineages can occur.

In our model, it is critical to determine how the mosaic-like environment is distributed in BM. To this end, we comprehensively examined 112 kinds of mosaic patterns, varying grains of area ratios among commitment areas supporting M, E, B and T. The strategy to generate the patterns is summarized in the ***Supplementary Note***. For each mosaic pattern out of 112 variants, we simulated that a single randomly located HSC in certain type of mosaic environment undergoes a certain round of cell division, and then undergo commitment according to the place they are located. After commitment, cells further make proliferation and finally terminal differentiation to form mature blood cells. For simplicity, the number of cell division before and after commitment is set as 5 and 5, respectively, in the simulation. We then investigated which cell lineages appeared, counting the number of cells belonging to each lineage. A total of 100 clones were simulated for each mosaic pattern. We found that simulation

based on 17 mosaic patterns resulted in histograms similar to the clinical data. Figure 6C shows a representative mosaic among them, and Figure 6D shows the histogram for the results of simulations in which a total of 256 of randomly located HSCs gave rise to hematopoietic colonies in the mosaic pattern shown in Figure 6C, which recapitulate the clinical results (Figure 6B). We also performed simulations of many virtual HSCs in the same mosaic environment while changing clone size (i.e. changing the cell division times before and after commitment, e.g. 3-3, 4-4, 5-5, 6-6, 7-7, resulting in the change in the size of the commitment sphere and the colony of mature cells). The relationship between clone size and number of lineages in each clone was then plotted in Figure 6E, which looks quite similar to Figure 6A. Thus, these simulations may have provided a reasonable explanation for the observed *in vivo* findings.

In the simulation, we assumed that T/NK cell progenitors and B cell progenitors are generated in distinct sites. If the induction site for T/NK cell progenitors is assumed to completely overlap or to be included as a part of B cell progenitor induction site (Figure 7A and B), our simulation predicts that “MET” type clones would hardly be generated (Figure 7C and D), which is not the actual case. Therefore, our *in vivo* findings together with the results of simulation strongly suggest that T/NK cell progenitors are produced in a different site from the one where B cell progenitors are produced.

Discussion

In the present study, by flow cytometrically detecting GPI-APs$^-$ cells in major six blood lineages, we have succeeded in visualizing the dynamics of individual HSCs in bone marrow failure patients. The results strongly suggest that most individual human HSCs only give rise to a limited range of hematopoietic progeny even in regular hematopoiesis.

We thought that we should provide a reasonable explanation for this unexpected finding i.e. the detection of GPI- APs$^-$ cells in the limited lineages over long period. Before we reach to our model, we have considered several possibilities to explain this finding, as briefly mentioned in the Result. Here we will discuss these possibilities, (a), (b), and (c).

(a) One possibility is that the limited lineage spectrum of progeny cells may reflect the presence of progenitors with equally limited potential. Indeed, in contrast to classical models of hematopoiesis, which assume the early segregation of HSCs to myelo-erythroid lineage and lymphoid lineage, some recent revised models of both mouse and human hematopoiesis have proposed that myeloid lineages are also derived from lymphoid branches[21, 22]. However, implications of these models in the present

study seem unlikely, since, as mentioned earlier, it is clear that most cases represent activities of self-renewing HSCs.

(b) Another simple explanation might be that HSCs are intrinsically heterogeneous in terms of developmental potential. Recent studies have shown such heterogeneity in murine HSCs, some being prone to produce myeloid cells while others to produce lymphoid cells[23-28]. However, it seems quite unlikely that HSC intrinsically have as many as 16 different subtypes as shown in Supplementary Table 1.

(c) It is also possible that the BM environment is heterogeneous in its ability to support the differentiation of distinct lineages. However, this is also quite unlikely. Provided that 400 stem cells contribute to whole hematopoiesis[1, 2] containing 18×10^{11} hematopoitic cells[29] in a total of about 1 kg active BM mass[30], the size of the hematopoietic site of one clone maintained by a single HSC in BM could be several cm^3, which may contain on the order of 10^9 hematopoietic cells and a comparable number of stromal cells. It is thus difficult to conceive that such large area contains only limited types of microenvironments.

Thus, we came to think that the above three explanations were quite unlikely. We then came to propose a reasonable model as an explanation of this phenomenon. This model assumes that the microenvironment of BM is mosaic in inducing the commitment

of progenitors to distinct lineages. If the size of area where uncommitted progenitors derived from one HSC can reach (“commitment sphere” in Figure 6C) is similar to the size of mosaic compartments, production of limited lineage cells can occur. We named our model “mosaic commitment-inducing microenvironment model”. This idea on first viewing may sound similar to the idea mentioned above in (c), but clearly different in that our model focuses on only commitment-inducing function of microenvironment and thus the size of mosaic area is much smaller. In this context, our model is also distinct from the classical idea of “hematopoietic inductive microenvironment (HIM)”[31], which is close to the idea mentioned above in (c).

To test whether our model can explain the *in vivo* findings, we applied a computer simulation approach, and simulations based on this model nicely recapitulated the observed *in vivo* findings. We emphasize here that we do not claim that our *in vivo* findings indicate the presence of mosaic commitment-inducing microenvironment in BM, but just propose a novel model that can explain the finding which otherwise is difficult to explain.

We recognize that the issue of whether the dynamics of HSCs observed in this study represents normal hematopoiesis must be critically discussed. Since the stable production of limited lineages was observed in milder cases of AA patients similarly to

more severe cases (Figure 2B), it is likely that these observed dynamics represent normal hematopoiesis. Detection of stable GPI-APs$^-$ clones producing limited lineages in healthy volunteers further supports this notion (Figure 5).

Nevertheless, here we will make discussion on the issue whether we are making some overestimation or underestimation in the interpretation of data in AA and MDS cases. Our findings can be summarized as follows: (i) A single HSC gives rise to a limited spectrum of lineage cells, (ii) HSCs stably and continuously produce blood cells by years.

As for the finding (i), the possibility could exist that GPI-APs$^-$ HSCs or progenitors have some defect in their migration potential, resulting in a failure to produce the complete spectrum of lineages. Although it is difficult to completely rule out this possibility, so far no published findings are available that support it. Another possible explanation could be that the HSCs in AA or MDS patients are already defective in developmental potential, or that the hematopoietic microenvironments in these patients are disorganized. However, these may not be critical factors, since detection of GPI-APs$^-$ cells of limited lineages was similarly seen in milder cases of AA, and also in healthy volunteers (Figure 2B, Figure 5). AA and MDS may result from various causes, and it has been supposed that a certain proportion of cases are primarily caused by the

impaired function of microenvironment. However, it is likely that in most cases in the present study the microenvironment itself is largely normal, because all the patients are bearing GPI-APs$^-$ cells, which is a sign to show that immunological pathophysiology is the main cause of the disease. It can also be noted that most AA patients who undergo allogeneic BM transplantation achieve complete hematologic recovery despite the fact that BM stromal cells are not transplantable[32], indicating that the hematopoietic microenvironments in AA patients are not impaired. Another possibility to be discussed is that the immunological reaction against GPI-APs$^-$ HSCs may affect their blood cell formation, since AA and MDS cases bearing GPI-APs$^-$ cells are thought to be caused by such autoimmune activities. However, such effect cannot be essential, since GPI-APs$^-$ cells are usually out of the target of immune cells, and the autoimmune activities in patients tested in this study have been virtually negligible, judging from the fact that the clone sizes of GPI-APs$^-$ cells in all patients scarcely changed during the observation periods.

We used antibody for CD55, CD59, or CD48 to positively stain GPI-AP expressing cells instead of FLAER that directly stain GPI-APs. In calibration experiments, we have seen that both methods virtually made no difference (data not shown). We note here that our approach could result in the overestimation of the presence of GPI-APs$^-$ cells

compared with the FLAER method, since FLAER can cover all GPI-APs. However, such overestimation seems to occur at a very low frequency, and moreover, it will never cause the underestimation for the presence of GPI-APs$^-$ cells.

Finding (ii) seems to fit well with the expected dynamics of HSCs. However, this finding could result from an overestimation. Since patients have some BM failure, the total HSC number may be more or less reduced. In such a less competitive situation, it could be that the active HSCs have a better chance to continue hematopoiesis. In addition, GPI-APs$^-$ cells may have some survival advantage over normal blood cells in patients because GPI-APs$^-$ cells may be less sensitive to immunological attacks than GPI-APs$^+$ cells[33]. However, in fact, the combination of GPI-APs$^-$ lineage as well as the proportion of GPI-APs$^-$ cells in PB persisted over a long period as it is, indicating that most of clones do not have an obvious dominance against other clones. It is also important to note that any possible overestimation in HSC longevity does not call into question finding (i).

Finally, it should be discussed whether such heterogeneity as proposed in our model can actually be observed in the BM environment. Heterogeniety of stromal environment has been pointed out in early studies for example based on the findings of preferential generation of erythroid or granulocytic cells in spleen and BM, respectively[31]. A recent

study has suggested the presence of a microenvironment that selectively supports B cell development in murine BM[34]. This then leads to the question of how large is the commitment sphere and mosaic fragments of the BM environment? We do not have any data concerning the actual size of the commitment sphere or compartments of mosaic environments, but would suggest that the relative size of these two may be similar to each other. Thus, each piece of the mosaic could be very small, containing only a few stromal cells. We hope that our present report and speculative model will facilitate further study on the distinct niches in BM environment.

Acknowledgements

This study was supported by Grant-in-Aids for Scientific Research from the Ministry of Education, Culture, Sports, Science and Technology of Japan (KAKENHI No.21390291, http://www.e-rad.go.jp/),a Grant-in-Aids from the Ministry of Health, Labor and Welfare of Japan. The calculations were performed by using the RIKEN Integrated Cluster of Clusters (RICC) facility.

Authorship Contributions

T.K., H.K. and T.N. were equally contributed to this work. H.K. and S.N. developed the concept of the study and supervised the project. T.K., T.N., H.K., K.I and M.O.-H. designed the experiments. T.K., T.N., Y.S. and K.H. performed the experiments and analyzed the data. T.K., H.K., T.N., S.O. and S.N. wrote the paper. All authors approved the final version of this paper.

Disclosure of Competing Financial Interests

All authors have no financial or personal relationships with other people or organizations that could inappropriately influence this study. The authors declare no competing financial interest. The funders had no role in study design, data collection and analysis, decision to publish, or preparation of the manuscript.

Author Information

Affiliations

Clinical Laboratory Science, Division of Health Sciences, Kanazawa University Graduate School of Medical Science, 5-11-80 Kodatsuno, Kanazawa, Ishikawa 920-0942 Japan.

Takamasa Katagiri and Shigeki Ohtake.

Cellular Transplantation Biology, Kanazawa University Graduate School of Medical Science, 13-1 Takaramachi, Kanazawa, Ishikawa 920-8640 Japan.

Ken Ishiyama, Yu Seiki, Kohei Hosokawa, and Shinji Nakao

Laboratory for Lymphocyte Development, RIKEN Research Center for Allergy and Immunology, 1-7-22 Sehiro-cho, Tsurumi-ku, Yokohama, Kanagawa 230-0045 Japan.

Hiroshi Kawamoto

Department of Mechanical Systems Engineering Faculty of Engineering, Kogakuin University, 1-24-2 Nishishinjuku, Shinjuku-ku, Tokyo 163-8677 Japan.

Takashi Nakakuki

Laboratory for Cellular Systems Modeling, RIKEN Research Center for Allergy and Immunology, 1-7-22 Sehiro-cho, Tsurumi-ku, Yokohama, Kanagawa 230-0045 Japan.

Mariko Okada-Hatakeyama

Corresponding Author

Correspondence and requests for materials should be addressed to S. Nakao

(snakao8205@staff.kanazawa-u.ac.jp).

References

1. Buescher ES, Alling DW, Gallin JI. Use of an X-linked human neutrophil marker to estimate timing of lyonization and size of the dividing stem cell pool. J Clin Invest. 1985;76:1581-1584.
2. Traulsen A, Pacheco JM, Luzzatto L, et al. Somatic mutations and the hierarchy of hematopoiesis. Bioessays.2010;32:1003-1008.
3. Wang H, Chuhjo T, Yasue S, et al. Clinical significance of a minor population of paroxysmal nocturnal hemoglobinuria-type cells in bone marrow failure syndrome. Blood. 2002;100:3897-3902.
4. Nishimura J, Inoue N, Wada H, et al. A patient with paroxysmal nocturnal hemoglobinuria bearing four independent PIG-A mutant clones. Blood. 1997;89:3470-3476.
5. Rosti V, Tremml G, Soares V, et al. Murine embryonic stem cells without pig-a gene activity are competent for hematopoiesis with the PNH phenotype but not for clonal expansion. J Clin Invest. 1997;100:1028-1036.
6. Maciejewski JP, Sloand EM, Sato T, et al. Impaired hematopoiesis in paroxysmal nocturnal hemoglobinuria/aplastic anemia is not associated with a selective proliferative defect in the glycosylphosphatidylinositol-anchored protein-deficient clone. Blood. 1997;89:1173-1181.
7. Araten DJ, Luzzatto L. The mutation rate in PIG-A is normal in patients with paroxysmal nocturnal hemoglobinuria (PNH). Blood. 2006;108:734-736.
8. Traulsen A, Pacheco JM, Dingli D. On the origin of multiple mutant clones in paroxysmal nocturnal hemoglobinuria. Stem Cells. 2007;25:3081-3084.
9. Dingli D, Luzzatto L, Pacheco JM. Neutral evolution in paroxysmal nocturnal hemoglobinuria. Proc Natl Acad Sci U S A. 2008;105:18496-18500.
10. Hillmen P, Lewis SM, Bessler M, et al. Natural history of paroxysmal nocturnal

hemoglobinuria. N Engl J Med. 1995;333:1253-1258.
11. Sugimori C, Mochizuki K, Qi Z, et al. Origin and fate of blood cells deficient in glycosylphosphatidylinositol-anchored protein among patients with bone marrow failure. Br J Haematol. 2009;147:102-112.
12. Sugimori C, Chuhjo T, Feng X, et al. Minor population of CD55-CD59- blood cells predicts response to immunosuppressive therapy and prognosis in patients with aplastic anemia. Blood. 2006;107:1308-1314.
13. Camitta BM, Thomas ED, Nathan DG, et al. A prospective study of androgens and bone marrow transplantation for treatment of severe aplastic anemia. Blood. 1979;53:504-514.
14. Bennett JM, Catovsky D, Daniel MT, et al. Proposals for the classification of the acute leukaemias. French-American-British (FAB) co-operative group. Br J Haematol. 1976;33:451-458.
15. Araten DJ, Nafa K, Pakdeesuwan K, et al. Clonal populations of hematopoietic cells with paroxysmal nocturnal hemoglobinuria genotype and phenotype are present in normal individuals. Proc Natl Acad Sci U S A. 1999;96:5209-5214.
16. Katagiri T, Qi Z, Ohtake S, et al. GPI-anchored protein-deficient T cells in patients with aplastic anemia and low-risk myelodysplastic syndrome: implications for the immunopathophysiology of bone marrow failure. Eur J Haematol. 2011;86:226-236.
17. Mochizuki K, Sugimori C, Qi Z, et al. Expansion of donor-derived hematopoietic stem cells with PIGA mutation associated with late graft failure after allogeneic stem cell transplantation. Blood. 2008;112:2160-2162.
18. Mayawala K, Vlachos DG, Edwards JS. Computational modeling reveals molecular details of epidermal growth factor binding. BMC cell biology. 2005;6:41.
19. Jayawardhana B, Kell DB, Rattray M. Bayesian inference of the sites of perturbations in metabolic pathways via Markov chain Monte Carlo. Bioinformatics. 2008;24:1191-1197.
20. Pu JJ, Hu R, Mukhina GL, et al. The small population of PIG-A mutant cells in myelodysplastic syndromes do not arise from multipotent hematopoietic stem cells. Haematologica. 2012;97:1225-33.
21. Kawamoto H, Katsura Y. A new paradigm for hematopoietic cell lineages: revision of the classical concept of the myeloid-lymphoid dichotomy. Trends Immunol. 2009;30:193-200.
22. Doulatov S, Notta F, Eppert K, et al. Revised map of the human progenitor hierarchy shows the origin of macrophages and dendritic cells in early lymphoid development. Nat Immunol. 2010;11:585-593.

23. Muller-Sieburg CE, Cho RH, Karlsson L, et al. Myeloid-biased hematopoietic stem cells have extensive self-renewal capacity but generate diminished lymphoid progeny with impaired IL-7 responsiveness. Blood. 2004;103:4111-4118.
24. Dykstra B, Kent D, Bowie M, et al. Long-term propagation of distinct hematopoietic differentiation programs in vivo. Cell Stem Cell. 2007;1:218-229.
25. Beerman I, Bhattacharya D, Zandi S, et al. Functionally distinct hematopoietic stem cells modulate hematopoietic lineage potential during aging by a mechanism of clonal expansion. Proc Natl Acad Sci U S A. 2010;107:5465-5470.
26. Morita Y, Ema H, Nakauchi H. Heterogeneity and hierarchy within the most primitive hematopoietic stem cell compartment. J Exp Med. 2010;207:1173-1182.
27. Cavazzana-Calvo M, Fischer A, Bushman FD, et al. Is normal hematopoiesis maintained solely by long-term multipotent stem cells? Blood. 2011;117:4420-4424.
28. Nakano T. Hematopoietic stem cells: generation and manipulation. Trends Immunol. 2003;24:589-594.
29. Osgood EE. Number and distribution of human hemic cells. Blood. 1954;9:1141-1154.
30. Pichardo JC, Trindade AA, Brindle JM, et al. Method for estimating skeletal spongiosa volume and active marrow mass in the adult male and adult female. J Nucl Med. 2007;48:1880-1888.
31. Trentin JJ. Determination of bone marrow stem cell differentiation by stromal hemopoietic inductive microenvironments (HIM). The American journal of pathology. 1971;65:621-628.
32. Awaya N, Rupert K, Bryant E, et al. Failure of adult marrow-derived stem cells to generate marrow stroma after successful hematopoietic stem cell transplantation. Experimental hematology. 2002;30:937-942.
33. Murakami Y, Kosaka H, Maeda Y, et al. Inefficient response of T lymphocytes to glycosylphosphatidylinositol anchor-negative cells: implications for paroxysmal nocturnal hemoglobinuria. Blood. 2002;100:4116-4122.
34. Kwon KR, Ahn JY, Kim MS, et al. Disruption of bis leads to the deterioration of the vascular niche for hematopoietic stem cells. Stem Cells. 2010;28:268-278.

Figure Legends

Figure 1. Detection of GPI-APs$^-$ cells in different lineages of blood cells.

A. One example of PB cells of a healthy individual having no GPI-APs$^-$ cells. B. GPI-APs$^-$ cell combination patterns in four patients. Profiles of PB cells of patients showing GPI-APs$^-$ cells in GMETNKB, GME, GMETNK and GMEB lineages are shown. Lineage markers used were CD11b for G, CD33 for M, glycophorin-A (CD235a) for E, CD3 for T, NKp46 for NK and CD19 for B. G, M, E, T, NK or B stands for granulocytes, monocytes, erythrocytes, T cells , NK cells or B cells, respectively.

Figure 2. Correlation between the clone size of GPI-APs$^-$ granulocytes and the number of cell lineages that contain GPI-APs$^-$ cells.

A. The percentage of GPI-APs$^-$ granulocytes and the number of cell lineages that contain GPI-APs$^-$ cells in individual patients are plotted. A red line for 0.25% stands for the expected value for an average size of a single HSC clone. B. The percentage of GPI-APs$^-$ granulocytes and the number of cell lineages that contain GPI-APs$^-$ cells in AA patients, classified in three categories according to the severity of disease (stage 1 or 2, stage 3, and stage 4 or 5), are plotted. AA patients were classified into five categories based on the disease severity (stage 1 or 2, stage 3, and stage 4 or 5) (for details, see

Supplementary Table 2).

Figure 3. The lineage combination pattern of GPI-APs$^-$ cells was same at the first sampling (A) and after 6 months (B).

Figure 4. The combination of GPI-APs$^-$ lineage as well as the proportion of GPI-APs$^-$ cells in PB persist over a long period.

GPI-APs$^-$ cells were analyzed in PB of 250 patients twice at intervals ranging 6 months to 18 months. The numbers 1 and 2 refer to the first and second analysis. In all cases, GPI-APs$^-$ cells were detected in the same lineages in both analyses. Among them, 25 cases (5 for each type of lineage combination) are shown. Bars represent the proportion of GPI-APs$^-$ cells in each lineage in PB.

Figure 5. GPI-APs$^-$ cells in healthy individuals.

A. Two healthy individuals (Healthy 1 and Healthy 2) showed GPI-APs$^-$ cells in the same lineage combination pattern at the first sampling (i) and 13 and 7 months after the first sampling (ii), respectively. B. The percentage of GPI-APs$^-$ granulocytes in the two healthy individuals are shown as closed circle in red . ◆, AA and MDS cases shown in

Figure 2A.

Figure 6. Simulation of HSC differentiation in a model assuming a mosaic environment for the commitment of primitive progenitors recapitulates the clinical observation.

A. The percentage of GPI-APs$^-$ granulocytes vs. the number of cell lineages in individual patients. Data from Figure 2A were re-plotted in a setting where granulocytes and monocytes were placed in the myeloid lineage and T and NK cell lineages in the T cell lineage. A red line for 0.25% stands for the expected value for an average size of a single HSC clone. B. Frequency of clone types among cases where the percentage of GPI-APs$^-$ granulocytes is between 0.3 to 3 %. C. A model assuming that the BM microenvironment is heterogeneous in supporting the commitment of progenitors. A certain range where the commitment of progenitors mainly occurs (with a probability of >97%) is termed the "commitment sphere" (see ***Supplementary Note*** for detailed information). Areas colored by beige, pink, light green, or blue represent the environment supporting commitment only towards M, E, T or B, respectively. If a HSC happens to reside in a location in which the commitment sphere contains only M and E regions, then this HSC can eventually produce only M and E cells, even if committed

progenitors expand enormously and become widely scattered. The depicted simulation goes as follows: a virtual HSC undergoes several cell divisions at fixed intervals while randomly migrating. The uncommitted progenitors then undergo a fate decision based on their ultimate location in the commitment sphere. Committed progenitors can also randomly move around, but can proliferate only in the lineage specific supporting environment. After several additional fixed time cell divisions as committed progenitors, cells become mature and lineage restricted. D. One example illustrating the frequency of clone types simulated as shown in (C). A total of 100 virtual HSCs were simulated to form hematopoietic clones, and numbers of the resulting clone types are illustrated (***Supplementary movies. 1-5***). E. Simulation of individual HCSs for size and number of progeny lineages. The simulation well recapitulated the clinical observations shown in (A).

Figure 7. Alternative conditions for induction sites to T and B cell lineages. Illustration of a mosaic pattern in a case where the induction site to the T lineage completely (A) or partially (B) overlaps with the B lineage (i.e. green area is for both T and B in (A), while blue are for T and green area for B in (B)). C and D. Histograms calculated from Panel A (C) or Panel B (D).

Supplementary Table Legends

Table S1. Classification of 16 different GPI-APs$^-$ cells patterns.

The lineage combinations of GPI-APs$^-$ cells in patients possessing GPI-APs$^-$ cells were classified into 16 different patterns.

Table S2. Definition of the AA severity.

We arbitrarily classified AA patients into five categories, namely stage 1, 2 and 3 (non severe), stage 4 (severe), and stage 5 (very severe), based on the severity of cytopenias.

Table S3. PIG-A gene mutations in each GPI-APs$^-$ cell population.

To confirm the clonal origin, GPI-APs$^-$ cells sorted from 5 patients were subjected to *PIG-A* gene analysis. The same mutation was identified in different lineages in 3 patients.

Supplementary Movie Legends

Movie S1.

Results as described in the supplementary note_Supplementary_Movie_1_for lineage type of METB.

Movie S2.

Results as described in the supplementary note_Supplementary_Movie_2_for lineage type of MET.

Movie S3.

Results as described in the supplementary note_Supplementary_Movie_3_for lineage type of MEB.

Movie S4.

Results as described in the supplementary note_Supplementary_Movie_4_for lineage type of ME.

Movie S5.

Results as described in the supplementary note_Supplementary_Movie_5_for lineage type of M.

Figures

Individual hematopoietic stem cells in human bone marrow of patients with aplastic anemia or myelodysplastic syndrome stably give rise to limited cell lineages

Short title: HSCs produce limited cell lineages

Takamasa Katagiri[1)2)*], Hiroshi Kawamoto[3)*], Takashi Nakakuki[4)*], Ken Ishiyama[2)], Mariko Okada-Hatakeyama[5)], Shigeki Ohtake[1)], Yu Seiki[2)], Kohei Hosokawa[2)] and Shinji Nakao[2)]

[1)] Clinical Laboratory Science, Division of Health Sciences, Kanazawa University Graduate School of Medical Science, 5-11-80 Kodatsuno, Kanazawa, Ishikawa 920-0942 Japan.
[2)] Cellular Transplantation Biology, Kanazawa University Graduate School of Medical Science, 13-1 Takara-machi, Kanazawa, Ishikawa 920-8640 Japan.
[3)] Laboratory for Lymphocyte Development, RIKEN Research Center for Allergy and Immunology, 1-7-22 Suehiro-cho, Tsurumi-ku, Yokohama, Kanagawa 230-0045 Japan.
[4)] Department of Mechanical Systems Engineering Faculty of Engineering, Kogakuin University, 1-24-2 Nishishinjuku, Shinjuku-ku, Tokyo 163-8677 Japan
[5)] Laboratory for Cellular Systems Modeling, RIKEN Research Center for Allergy and Immunology, 1-7-22 Suehiro-cho, Tsurumi-ku, Yokohama, Kanagawa 230-0045 Japan.

* T.K., H.K. and T.N. were equally contributed to this work.

Corresponding to:
Shinji Nakao (snakao8205@staff.kanazawa-u.ac.jp)
Cellular Transplantation Biology, Kanazawa University Graduate School of Medical Science, 13-1 Takara-machi, Kanazawa, Ishikawa 920-8640 Japan.

Figure 1. Detection of GPI-APs$^-$ cells in different lineages of blood cells.
Figure 2. Correlation between the clone size of GPI-APs$^-$ granulocytes and the number of cell lineages that contain GPI-APs$^-$ cells.
Figure 3. The lineage combination pattern of GPI-APs$^-$ cells was same at the first sampling (A) and after 6 months (B).
Figure 4. The combination of GPI-APs$^-$ lineage as well as the proportion of GPI-APs$^-$ cells in PB persist over a long period.
Figure 5. GPI-APs$^-$ cells in healthy individuals.
Figure 6. Simulation of HSC differentiation in a model assuming a mosaic environment for the commitment of primitive progenitors recapitulates the clinical observation.
Figure 7. Alternative conditions for induction sites to T and B cell lineages.

Figure 1

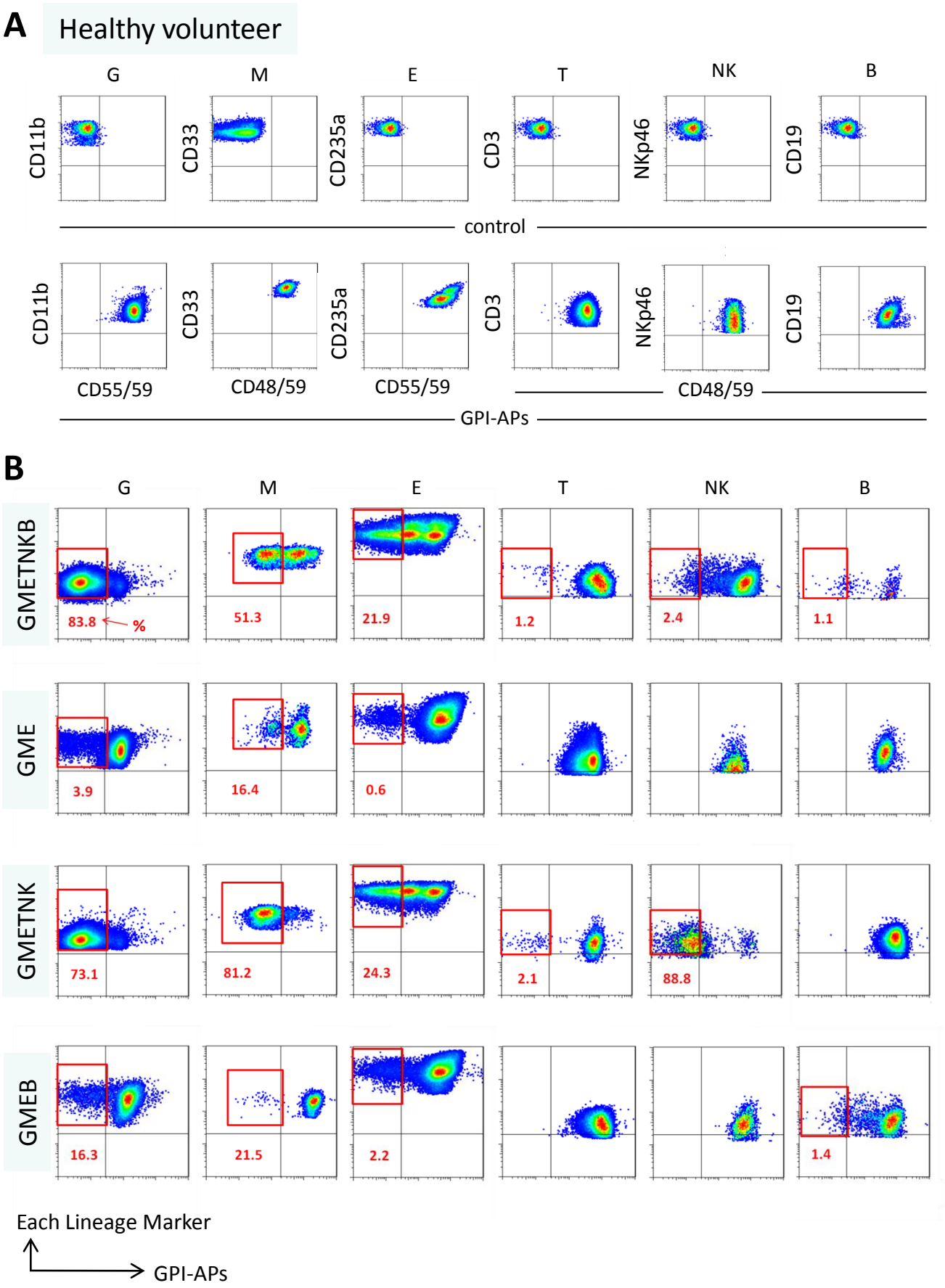
A
Healthy volunteer
G
M
E
T
NK
B
CD11b
CD33
CD235a
CD3
NKp46
CD19
control
CD55/59
CD48/59
CD55/59
CD48/59
GPI-APs
B
G
M
E
T
NK
B
GMETNKB
83.8
%
51.3
21.9
1.2
2.4
1.1
GME
3.9
16.4
0.6
GMETNK
73.1
81.2
24.3
2.1
88.8
GMEB
16.3
21.5
2.2
1.4
Each Lineage Marker
GPI-APs

Figure 2

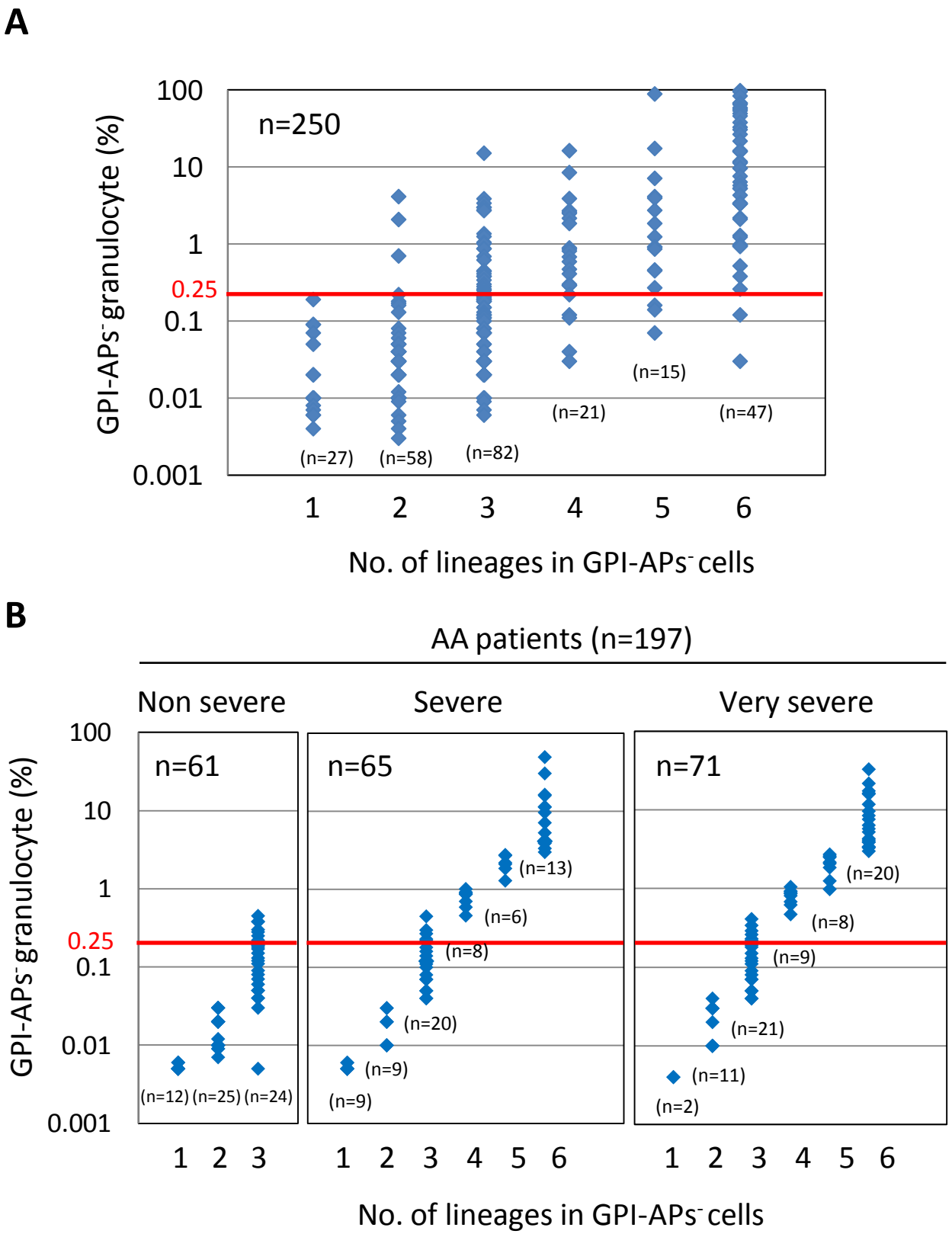
A
n=250
100
10
1
0.25
0.1
0.01
0.001
GPI-APs- granulocyte (%)
(n=27)
(n=58)
(n=82)
(n=21)
(n=15)
(n=47)
1
2
3
4
5
6
No. of lineages in GPI-APs- cells
B
AA patients (n=197)
Non severe
Severe
Very severe
n=61
n=65
n=71
(n=12)
(n=25)
(n=24)
(n=9)
(n=9)
(n=20)
(n=8)
(n=6)
(n=13)
(n=2)
(n=11)
(n=21)
(n=9)
(n=8)
(n=20)
No. of lineages in GPI-APs- cells

Figure 3

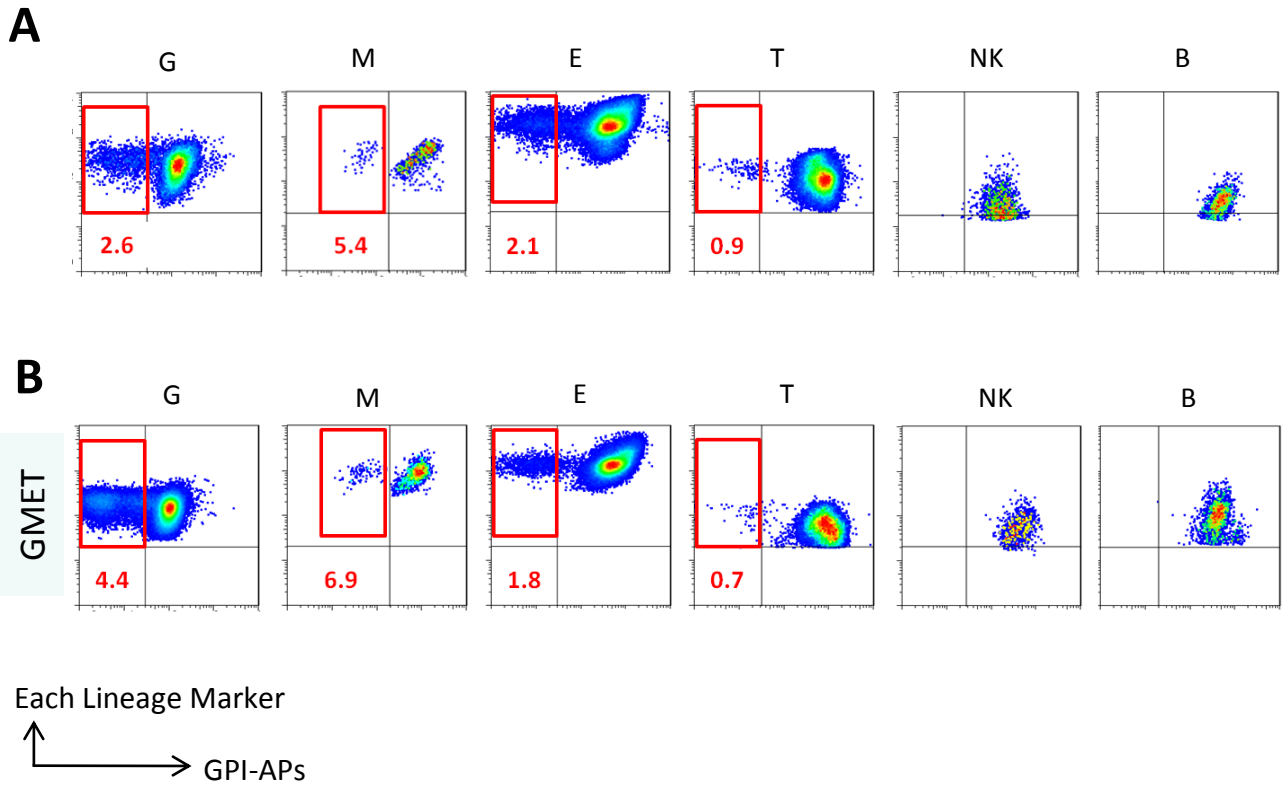
A
G
M
E
T
NK
B
2.6
5.4
2.1
0.9
B
G
M
E
T
NK
B
GMET
4.4
6.9
1.8
0.7
Each Lineage Marker
GPI-APs

Figure 4

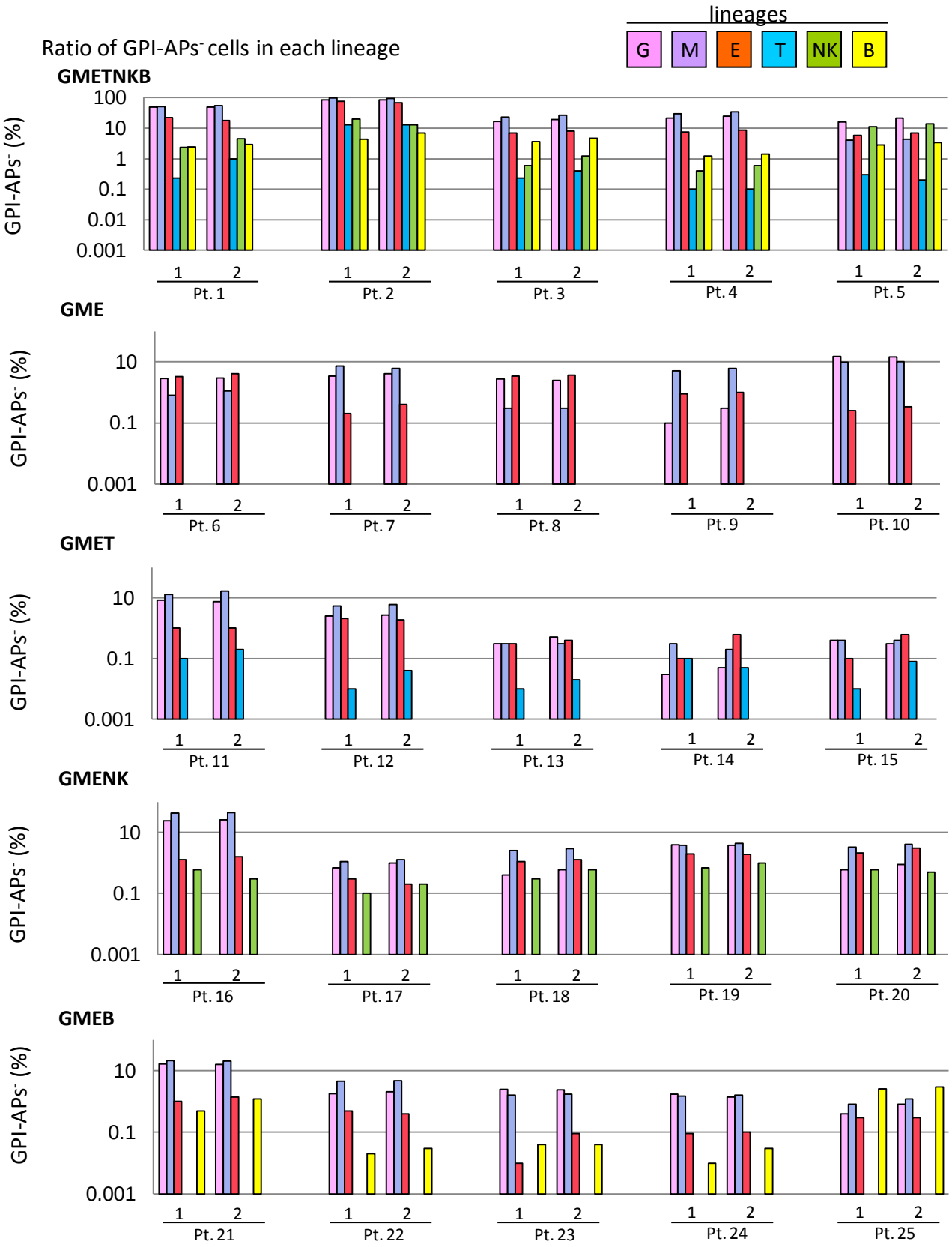
Ratio of GPI-APs- cells in each lineage
lineages
G
M
E
T
NK
B
GMETNKB
GPI-APs- (%)
100
10
1
0.1
0.01
0.001
1
2
Pt. 1
Pt. 2
Pt. 3
Pt. 4
Pt. 5
GME
10
0.1
0.001
Pt. 6
Pt. 7
Pt. 8
Pt. 9
Pt. 10
GMET
Pt. 11
Pt. 12
Pt. 13
Pt. 14
Pt. 15
GMENK
Pt. 16
Pt. 17
Pt. 18
Pt. 19
Pt. 20
GMEB
Pt. 21
Pt. 22
Pt. 23
Pt. 24
Pt. 25

Figure 5

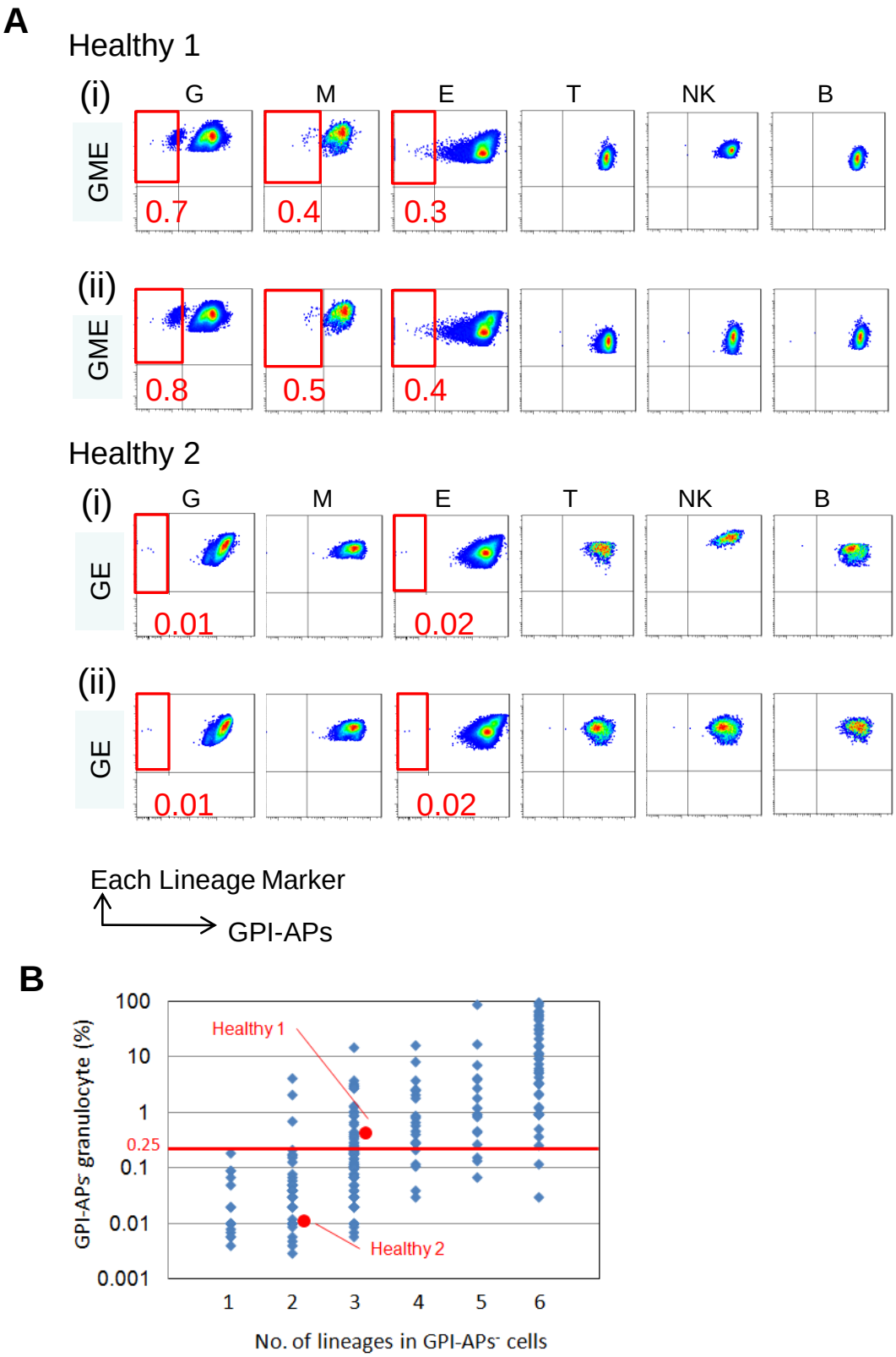
A
Healthy 1
(i)
G
M
E
T
NK
B
GME
0.7
0.4
0.3
(ii)
GME
0.8
0.5
0.4
Healthy 2
(i)
G
M
E
T
NK
B
GE
0.01
0.02
(ii)
GE
0.01
0.02
Each Lineage Marker
GPI-APs
B
GPI-APs⁻ granulocyte (%)
100
10
1
0.25
0.1
0.01
0.001
Healthy 1
Healthy 2
1
2
3
4
5
6
No. of lineages in GPI-APs⁻ cells

Figure 6

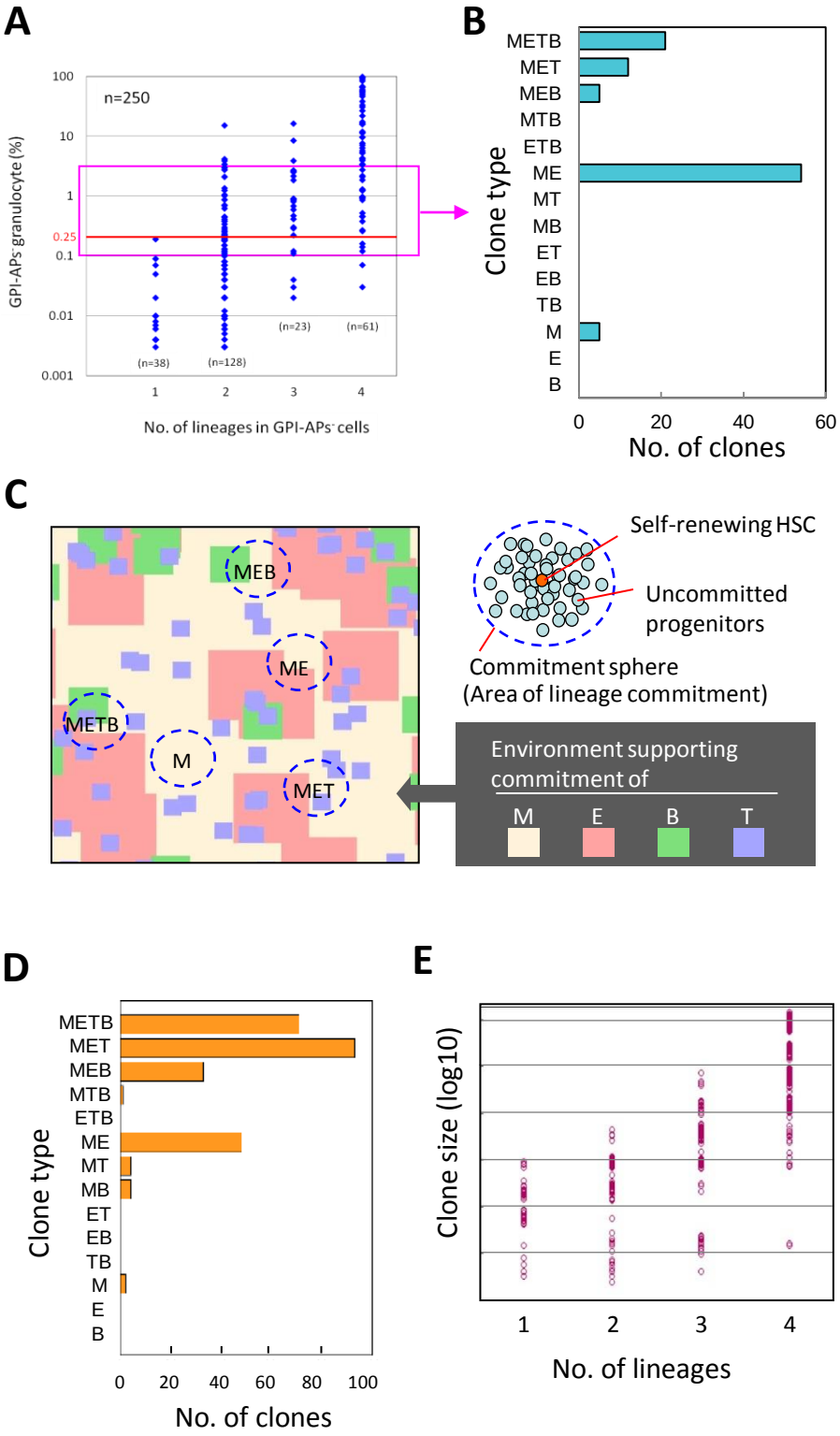
A
n=250
GPI-APs granulocyte (%)
100
10
1
0.25
0.1
0.01
0.001
(n=38)
(n=128)
(n=23)
(n=61)
1
2
3
4
No. of lineages in GPI-APs- cells
B
METB
MET
MEB
MTB
ETB
ME
MT
MB
ET
EB
TB
M
E
B
Clone type
0
20
40
60
No. of clones
C
MEB
ME
METB
M
MET
Self-renewing HSC
Uncommitted progenitors
Commitment sphere
(Area of lineage commitment)
Environment supporting commitment of
M
E
B
T
D
METB
MET
MEB
MTB
ETB
ME
MT
MB
ET
EB
TB
M
E
B
Clone type
0
20
40
60
80
100
No. of clones
E
Clone size (log10)
1
2
3
4
No. of lineages

Figure 7

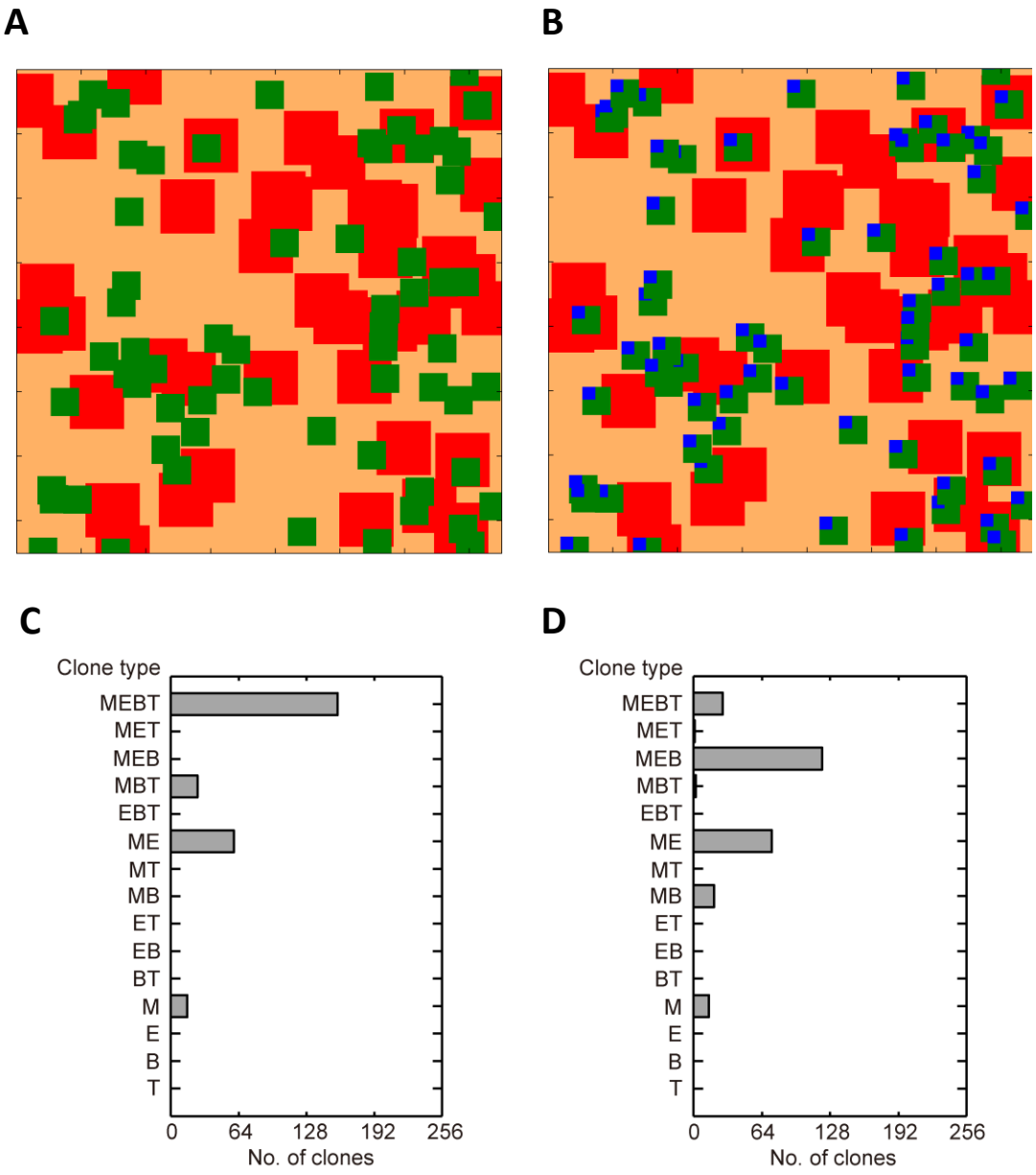
A
B
C
D
Clone type
MEBT
MET
MEB
MBT
EBT
ME
MT
MB
ET
EB
BT
M
E
B
T
0
64
128
192
256
No. of clones
Clone type
MEBT
MET
MEB
MBT
EBT
ME
MT
MB
ET
EB
BT
M
E
B
T
0
64
128
192
256
No. of clones